16. Nayak V U, Edwards D O, Masuhara N *Phys. Rev. Lett.* **50** 990 (1983)
17. Anderson A et al. *Phys. Rev. A* **34** 3513 (1986)
18. Stern O *Naturwissenschaften* **17** 391 (1929)
19. Frish R, Stern O *Z. Phys.* **84** 430 (1933)
20. Keith D W et al. *Phys. Rev. Lett.* **61** 1580 (1988)
21. Berkhout J J et al. *Phys. Rev. Lett.* **63** 1689 (1989)
22. Carnal O, Faulstich A, Mlynek J *App. Phys. B* **53** 88 (1991)
23. Carnal O, Mlynek J *Phys. Rev. Lett.* **66** 2689 (1991)
24. Keith D W et al. *Phys. Rev. Lett.* **66** 2693 (1991)
25. Friedburg H, Paul W *Naturwissenschaften* **37** 20 (1950)
26. Friedburg H, Paul W *Naturwissenschaften* **38** 159 (1951)
27. Korsunskii M I, Fogel' Ya M *Zh. Eksp. Teor. Fiz.* **21** 25 (1951); **21** 38 (1951)
28. Vanthier R *C.R. Acad. Sci.* **228** 1113 (1949)
29. Goldenberg H M, Kleppner D, Ramsey N F *Phys. Rev. Lett.* **5** 361 (1960)
30. Bennewitz H G, Paul W, Schlier Ch *Z. Phys.* **141** 6 (1955)
31. Gordon J P, Zeiger H J, Townes C H *Phys. Rev.* **99** 1264 (1955)
32. Basov N G, Prokhorov A M *Zh. Eksp. Teor. Fiz.* **28** 249 (1955) [*Sov. Phys. JETP* **1** 184 (1955)]
33. Askar'yan G A *Zh. Eksp. Teor. Fiz.* **42** 1567 (1962) [*Sov. Phys. JETP* **15** 1088 (1962)]
34. Letokhov V S *Pis'ma Zh. Eksp. Teor. Fiz.* **7** 348 (1968) [*JETP Lett.* **7** 272 (1968)]
35. Salomon C et al. *Phys. Rev. Lett.* **59** 1659 (1987)
36. Balykin V I et al. *Opt. Lett.* **13** 958 (1988)
37. Chu S et al. *Phys. Rev. Lett.* **55** 48 (1985)
38. Meacher D R *Contemp. Phys.* **39** 329 (1998)
39. Bjorkholm J E et al. *Phys. Rev. Lett.* **41** 1361 (1978)
40. Ashkin A, Dziedzic J M *Science* **235** 1517 (1987)
41. Hänsch T W, Schawlow A L *Opt. Commun.* **13** 68 (1975)
42. Wineland D J, Dehmelt H *Bull. Am. Phys. Soc.* **20** 637 (1975)
43. Prentiss M et al. *Appl. Phys. Lett.* **60** 1027 (1992); Timp G et al. *Phys. Rev. Lett.* **69** 1636 (1992)
44. McClelland J J et al. *Science* **262** 877 (1993)
45. Bradley C C et al. *Appl. Surf.* **141** 210 (1999)
46. McClelland J J, Prentiss M, in *Nanotechnology* (Ed. G Timp) (New York: AIP Press/Springer, 1999) Ch. 10
47. Oberthaler M K, Pfau T *J. Phys. Condens. Matter* **15** R233 (2003)
48. Meschede D, Metcalf H *J. Appl. Phys. D.: Appl. Phys.* **36** R17 (2003)
49. McClelland J J et al. *Sci. Technol. Adv. Mater.* **5** 575 (2004)
50. Mützel M, Haubrich D, Meschede D *Appl. Phys. B* **70** 689 (2000)
51. Balykin V I et al. *Zh. Eksp. Teor. Fiz.* **90** 458 (1986) [*Sov. Phys. JETP* **63** 264 (1986)]
52. Schulze Th et al. *Appl. Phys. Lett.* **78** 1781 (2000); Schulze Th et al. *Appl. Phys. B* **70** 671 (2001)
53. Cohen-Tannoudji C, Phillips W *Phys. Today* **43** (10) 33 (1992)
54. Gupta R et al. *Appl. Phys. Lett.* **67** 1378 (1995); *Phys. Rev. Lett.* **76** 4689 (1996)
55. Berggren K K et al. *Science* **269** 1255 (1995)
56. Behringer R E, Natarajan V, Timp G *Opt. Lett.* **22** 114 (1997)
57. Drodofsky U et al. *Appl. Phys. B* **65** 755 (1997)
58. Jurdik E et al. *Phys. Rev. B* **69** 201102 (2004)
59. Mützel M et al. *Appl. Phys. B* **77** 1 (2003)
60. te Sligte E et al. *Microel. Eng.* **67 – 68** 664 (2003)
61. Myszkiewicz G et al. *Appl. Phys. Lett.* **85** 3842 (2004)
62. te Sligte E et al. *Appl. Phys. Lett.* **85** 4493 (2004)
63. Ohmukai R, Urabe S, Watanabe M *Sci. Technol. Adv. Mater.* **5** 585 (2004)
64. Rehse S J, McGowan R W, Lee S A *Appl. Phys. B* **70** 657 (2000)
65. Johnson K S et al. *Appl. Phys. Lett.* **69** 2773 (1996)
66. Rehse S J et al. *Appl. Phys. Lett.* **71** 1427 (1997)
67. Balykin V I *Adv. Atom. Mol. Opt. Phys.* **41** 181 (1999)
68. Balykin V I, Klimov V V, Letokhov V S *J. Physique II* **4** 1981 (1994)
69. Lüthi R et al. *Appl. Phys. Lett.* **75** 1314 (1999)
70. Subbotin M V, Balykin V I, Laryushin D V, Letokhov V S *Opt. Commun.* **139** 107 (1997)
71. Balykin V I et al. *Pis'ma Zh. Eksp. Teor. Fiz.* **84** 544 (2006) [*JETP Lett.* **84** 466 (2006)]
72. Oberst H, Kasashima S, Balykin V I, Shimisu F *Phys. Rev. A* **68** 013606 (2003)
73. Bradley C C, Anderson W R, McClelland J J, Celotta R J *Appl. Surf. Sci.* **141** 210 (1999)
74. Li Y T et al. *Phys. Rev. E* **69** 036405 (2004)
75. Melentiev P N et al. *Nano Lett.* (2009) (submitted)

PACS numbers: **32.30.–r**, 32.30.Jc, 42.82.Cr, 95.30.Ky, **97.10.–q**
DOI: 10.3367/UFNe.0179.200903j.0305

Spectroscopy of ionized atoms for astrophysics and nanotechnology

A N Ryabtsev, S S Churilov

1. Introduction

Spectroscopy of ionized atoms is an important tool in the solution of scientific and technological problems in different fields of physics. The results of investigations of ion spectra were and are used in solar and stellar research, for the diagnostics of laboratory plasma sources, including the controlled thermonuclear fusion problem, and for high-resolution optical microscopy and lithography. The Department of Atomic Spectroscopy of the Institute of Spectroscopy, RAS (ISAN) has been pursuing research in the majority of these areas since the inception of the institute. The Department now has a unique experimental, theoretical, and methodological basis sufficient for analyzing the most complex ion spectra and validly applying the data acquired. In this report, we consider two relatively distant areas of application of the spectroscopy of ionized atoms: investigations into the atmospheres of peculiar magnetic stars and the development of efficient optical lithography sources in the far vacuum ultraviolet (VUV) domain.

A group of stars relatively close in properties, whose spectra exhibit high-intensity absorption lines of heavy elements, which are quite weak or not recorded at all in the spectra of the main-sequence stars, have long been the particular concern of astrophysicists. Absorption lines of rare-earth ions, and sometimes of heavier elements up to Pt, Bi, and U, are recorded in the stellar atmospheres of this group. The masses of these stars range from 2 to 5 solar masses, their surface temperatures lie between 7000 – 18000 K, and most of them have high magnetic fields up to 10 – 30 kGs, strong atmospheric turbulence, and pulsating intensities in their absorption spectra. These objects are known as peculiar magnetic stars and are often referred to as Ap stars in the literature. The atoms of rare-earth elements in the atmospheres of these stars are primarily in the first and second ionization stages, whose spectra have not been adequately studied [1 – 3]. In many spectra, especially in the spectra of doubly ionized atoms, only several tens (out of several thousand possible) lines lying in the visible range (transitions between low levels) have been identified. The transition probabilities (line strengths) calculated for doubly ionized rare-earth atoms and stored in DREAM (Database on Rare Earths at Mons University) [3] are restricted to the transition probabilities between a small number of the known energy levels. Determining the composition and parameters of the atmospheres of Ap stars, defining relevant processes more precisely, and accounting for the emergence of their special features requires data, as comprehensive as possible, about the corresponding ion spectra, which are practically the only source of information about these objects. In Section 2, we describe investigations into the spectra of doubly ionized atoms Nd III and Eu III and the application of the findings of this research to the diagnostics of Ap stars.

Another topical application area of investigations into complex ion spectra is projection optical lithography in the extreme VUV domain. At present, integrated microcircuits are produced using the radiation of excimer ArF lasers ($\lambda = 193$ nm). To further upgrade the microcircuit parameters (increase the number of active elements in microprocessors and improve the internal performance, memory space, etc.) requires advancing to the shorter-wavelength range. Moving to the extreme VUV range will allow bringing the spatial resolution of optical lithography to 10 nm, which will undoubtedly result in a new leap in the development of microelectronics, up to its possible renaming to 'nanoelectronics.' The last several years have seen the vigorous development of a high-efficiency lithography source at the wavelength $\lambda = 13.5$ nm coinciding with the reflection band of Mo/Si mirrors. Plasma sources like vacuum sparks and laser-produced plasmas containing tin ions are believed to hold the greatest promise. These ions have a very intense emission peak near $\lambda = 13.5$ nm, which consists of a very large array of 4–4 transitions in several ions with an open 4d subshell (see, e.g., Refs [4, 5]). But the spectroscopic data on these transitions, which are extremely important for optimizing lithographic source parameters, have been practically nonexistent. In Section 3, we outline the results of tin ion spectra investigations with an eye to the development of a source for 13.5 nm lithography.

2. Investigation of the spectra of doubly ionized rare-earth elements for astrophysics

Nd III ion. The available data on the Nd III spectrum have been highly disembodied and partly contradictory [1, 6, 7]. This disagreement led to substantial complications in the analysis of the chemical composition of Ap stars [8]. Our group, jointly with the Institute of Astronomy, RAS, carried out an independent analysis of the Nd III spectrum with the use of the spectrum of the HD 217522 Ap star in the visible range. This star has a relatively low magnetic field ($B_s < 2$ kGs), and therefore the line profiles in its spectrum are hardly distorted by the Zeeman splitting and their wavelengths in the visible range are measured with high precision ($\sim 5 \times 10^{-4}$ nm) [9]. The energies and transition probabilities for the Nd III spectrum were calculated by the Hartree–Fock technique with the use of Cowan's code package [10]. In these calculations, we took the strong interaction between the electron configurations $4f^4 + 4f^3 6p + 4f^2 5d^2$ and $4f^3 5d + 4f^3 6s + 4f^2 5d 6p$ into account (hereinafter, we omit the completely filled electron subshells in the notation for configurations). As far as possible, the interaction integrals were scaled with the inclusion of the data resulting from the analysis of the spectra of other doubly ionized atoms of rare-earth elements. More than 70 spectral lines were identified and about 40 energy levels of the $4f^4$ and $4f^3 5d$ configurations were determined in the course of this analysis. The classified transitions are shown with the darker color in Fig. 1, which shows the total calculated spectrum of the $4f^4 - 4f^3(5d + 6s) - 4f^3 6p$ transitions in Nd III. It can be seen that the identified transitions are only a very small part of the Nd III spectrum. However, even with the help of such an incomplete analysis, it was possible to confidently determine the density of neodymium in the

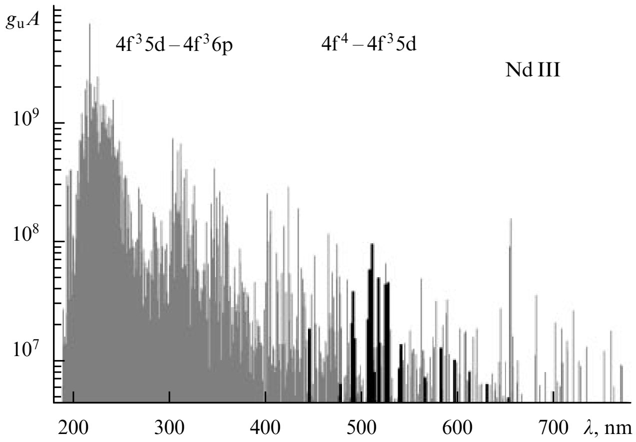

Figure 1. The calculated $4f^4 - 4f^3 5d - 4f^3 6p$ transition spectrum in Nd III. The line intensities are given in units of $g_u A$, where A is the radiative transition probability in [s^{-1}] and g_u is the statistical weight of the upper transition level. The darker color indicates the classified transitions.

atmosphere of the star HD 144897, in which all the rare-earth elements from La to Lu, with the exception of unstable Pm, were discovered in [8]. A portion of the spectrum of this star with Nd III lines and the result of its parametric modeling are depicted in Fig. 2. The newly obtained data on the Nd III spectrum allowed calculating the absorption spectrum of the stellar atmosphere with high precision. The observed structures of the Zeeman line splitting corresponding to the magnetic intensity of the HD 144897 star also confirm the validity of the Nd III spectrum analysis conducted.

Eu III ion. An analysis of the very complicated spectrum of Eu III is critical to the investigation of stellar atmospheres, because Europium is most abundant in the atmospheres of hot Ap stars, where it is found primarily in the second ionization stage (Eu III) [11, 12]. The spectrum of Eu III has been studied much better than that of Nd III: a list of its 890 lines has been published, one-third of them being classified as transitions between the levels $4f^7$, $4f^6(^7F)5d$, $4f^6(^7F)6s$, and $4f^6(^7F)6p$ [13]. But the transition probabilities calculated from the Eu III spectrum identification data turned out to be 2–3 orders of magnitude lower than those

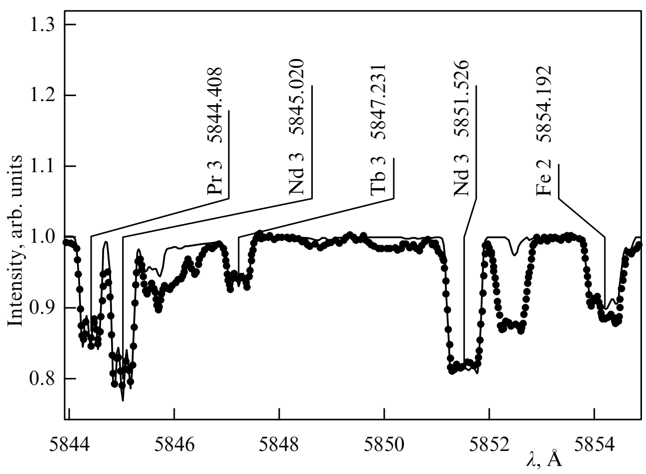

Figure 2. Portion of the atmospheric absorption spectrum of the HD 144897 peculiar magnetic star (points) and the result of its simulation (continuous line). Borrowed from Ref. [8].

Table 1. Densities, $\log(N/N_{\rm tot})$, of rare-earth elements in the atmospheres of several Ap stars and the Sun measured from the spectra of different ions. Measurement errors are given in parentheses. (Borrowed from Ref. [8].)

Ion	HD 144897	HD 170973	HD 116458	Sun
Ce II	−6.69(20)	−6.87	−7.34	−10.46
Ce III	−6.64(18)			
Pr II	−6.60(14)	−7.19	−7.30	−11.33
Pr III	−6.69(14)	−6.87	−7.32	
Nd II	−6.45(12)	−6.48		−10.59
Nd III	−6.45(20)	−6.63	−7.26	
Sm II	−6.98(21)	−7.07		−11.03
Sm III	−6.92(20)			
Eu II	**−7.75(20)**	**−7.77**	**−7.94**	**−11.52**
Eu III	**−6.32(23)**		**−6.90**	
Cd II	−6.95(18)	−7.17	−7.47	−10.92
Cd III	−6.60(14)			
Tb II	−7.83(10)			−11.76
Tb III	−7.92(22)	−7.96		
Dy II	−7.12(22)	−7.17		−10.90
Dy III	−6.99(39)	−7.13		
Er II	−7.55(14)	−7.54		−11,11
Er III	−7.21(14)	−7.79		
Tm II	−8.12(20)			−12.04
Tm III	−7.70(20)			

that would be expected from the lifetime measurements for some Eu III levels [14] and from astrophysical data [15].

The densities of several rare-earth elements in the atmospheres of three Ap stars, which were determined from the second and third spectra under the assumption of a local thermodynamic equilibrium, are collected in Table 1 [8]. It can be seen that the densities measured from the lines of different multiplicity ions are consistent, to within the uncertainty of measurements, for all the elements, with the exception of Europium. The densities of Europium derived from the spectra of Eu II and Eu III diverge by more than an order of magnitude. To solve this problem, new Eu III spectrum calculations were undertaken using the generalized least-square method (see, e.g., Refs [16, 17]) with the scaling of Hartree – Fock integrals and the inclusion of the effects of interaction with highly excited configurations.

The radial integrals were scaled with the inclusion of the data obtained in the analysis of the spectra of other doubly ionized lanthanides with the level lifetimes known from experiments. Along with the $4f^7$, $4f^6 5d$, $4f^6 6s$, and $4f^6 6p$ configurations under investigation, the doubly excited $4f^5 5d^2$, $4f^5 5d6s$, $4f^5 6s^2$, $4f^5 5d6p$, and $4f^5 6s6p$ configurations, which interact with them, were also included in the calculations. The transition probabilities calculated in this way are in good agreement with the measured level lifetime data and with the probabilities stored in DREAM [3]. In this case, the discrepancy between the Europium densities derived from the spectra of Eu II and Eu III became two times smaller. The residual difference may well be attributed to the deviation of level populations from the equilibrium values in Ap stellar atmospheres [18].

The calculations also resulted in the classification of 90 new spectral lines and the determination of more than 30 new energy levels in the spectrum of Eu III [19]. The list of calculated transition probabilities for the 200 – 1000 nm wavelength range now contains 1145 lines arising from transitions between the known levels and 23,800 lines arising from transitions between all levels with energies lower than 90,000 $\rm cm^{-1}$. The results of these identifications and calculations were entered into the Vienna Atomic Line Database (VALD).

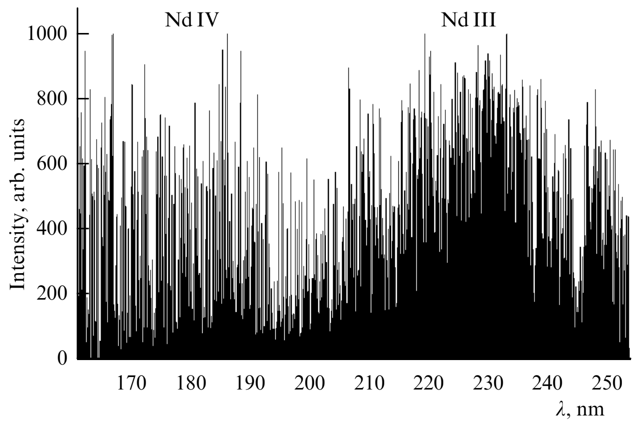

Figure 3. High-resolution spectrum of neodymium ions from a low-voltage spark plasma recorded with ISAN's VUV spectrograph.

We note that the results outlined in this section were derived from the spectrograms recorded in the visible spectral range. However, the strongest transitions of doubly ionized atoms of rare-earth elements lie in the VUV spectral domain (see, e.g., Fig. 1). Investigating the VUV spectra of rare-earth ions would permit obtaining a wealth of reliable information about the processes occurring in the atmospheres of hot stars.

Planned for 2010 is the launch of the World Space Observatory (WSO), which will accommodate a high-resolution spectrometer WSO/UV for the 102 – 310-nm wavelength range. Recording the spectra of peculiar magnetic stars will inevitably bring up the question about the availability of laboratory data on the spectra of doubly and triply ionized heavy atoms. These data may be obtained using the normal-incidence VUV ISAN spectrograph, which outperforms the WSO/UV spectrometer. For example, Fig. 3 shows a spectrum of neodymium ions in the 160 – 250 nm wavelength range, which was recorded with a resolution of 200000 with ISAN's spectrograph. Standing out in the spectrum are line arrays arising from the $4f^3 5d - 4f^3 6p$ transitions in Nd III (cf. Fig. 1) and the resonance $4f^3 - 4f^2(5d + 6s)$ transitions in Nd IV. Presently, an analysis is being made of neodymium and ytterbium spectra below 250 nm, which were recorded in circumstances where the excitation of doubly and triply ionized atoms was dominant.

3. Investigation of tin ion spectra for extreme VUV lithography

As noted in the Introduction, developing a high-efficiency optical 13.5 nm lithography source requires comprehensive investigations into the spectra of multiply charged tin ions. According to preliminary calculations, the $4d^m - (4p^5 4f^{m+1} + 4d^{m-1} 4f)$ transitions ($m = 1 - 5$) in the spectra of Sn X – Sn XIV produce an intense radiation peak near the wavelength 13.5 nm. These transitions contain a multitude of closely located lines, and hence only a spectrally unresolved structure of the 13.5 nm peak had been observed in the spectra recorded previously (see, e.g., Ref. [5]).

These 4–4 type transitions, which lie aside the main peak in the $\lambda > 16$ nm domain, were studied only for low-multiplicity ions: Sn VI [20] and Sn VII [21]. In the 13–14 nm wavelength range, only the four strongest 4–4 transition lines were classified in the simplest Sn XIV spectrum ($m = 1$) [22]. The spectra of analogous transitions in the nearest members of the corresponding isoelectronic sequences were not known either. That is why the 4–4 transitions were investigated via extrapolation along the 'isonuclear' sequence of tin ions with different multiplicities. The spectra were calculated by the Hartree–Fock method with the use of Cowan's code package [10] and the inclusion of $4d^m$, $4d^{m-1}nl$ ($n = 5, 6$; $l = $ s, p, d, f), $4p^5 4d^{m+1}$, and $4p^5 4d^m 5s$ configurations.

The spectra were excited in a low-inductance vacuum spark with the peak discharge current $I = 10-25$ kA and recorded with a DFS-26 grazing-incidence spectrograph equipped with a holographic grating (3600 grooves/mm). The resolving power of this instrument is equal to about 20000 in the $\lambda = 13-14$ nm region, which enabled the structure of the strongest 4–4 transitions to be spectrally resolved. Figure 4 shows the spectra of tin ions acquired for the discharge currents 15 and 20 kA. Each spectrum consists of approximately 1000 strong lines, which stand out against a quasicontinuous background made up of a multitude of less intense lines. The calculated positions of highest-intensity transitions in different tin spectra are indicated in Fig. 4a. We can see that the spectral lines of different ions can be selected according to the dependence of their intensities on the discharge current. In particular, on decreasing the current from 20 to 15 kA, the Sn VIII line intensities increase substantially, while the Sn XIII–XIV lines decrease. This fact was taken into account in the classification of the spectra.

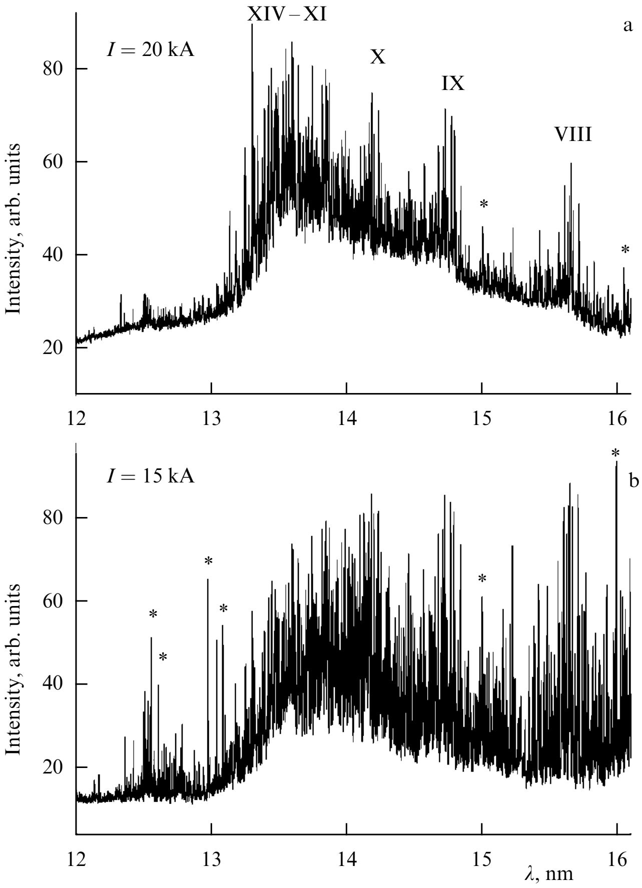

Figure 4. Extreme VUV spectra of tin ions excited in a low-inductance vacuum spark plasma. (Borrowed from Ref. [26].) Asterisks indicate oxygen and aluminum impurity ion lines.

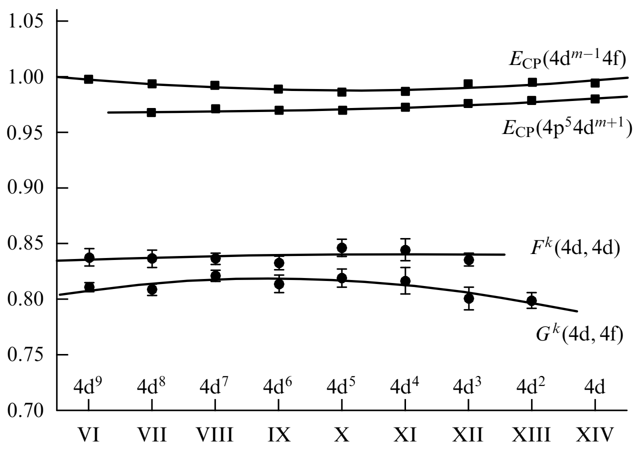

Figure 5. Variation of the scaling factors for the energy parameters of the $4d^{m-1}4f$ and $4p^5 4d^{m+1}$ configurations along the isonuclear sequence of tin ions.

The spectra were analyzed in several steps. Initially, the $4d^7 - (4p^5 4d^8 + 4d^6 4f)$ transitions were investigated in the spectrum of Sn VIII with the known structure of the ground configuration $4d^7$ [23]. In the semiempirical processing of the data acquired, it was noted that the scaling factors (the ratios between the semiempirical energy parameters and their Hartree–Fock values) were practically constant along the isonuclear sequence Sn VI–VIII [24]. That is why at the next stages, the spectra were analyzed by means of extrapolation of the scaling factors to their values for higher-charged ions. We thus classified the 4–4 transitions in the relatively simple spectra of Sn XIII and Sc XIV [25], and then investigated the higher-complexity spectra of Sn IX–Sn XII [26]. In the latter spectra, it has been possible to classify only the most intense transitions; however, even this incomplete analysis permitted determining the semiempirical values of the main parameters with sufficient precision. Figure 5 shows the scaling factors for the average energies (E_{CP}) and Slater parameters determined by the analysis of the excited configurations $4f^{m-1}4f$ and $4p^5 4d^{m+1}$ for the spectra of the isonuclear sequence Sn VI–XIV. The dependence of each factor on the nuclear charge is approximated by second-degree polynomials, up to uncertainties in the determination of the parameters (the uncertainty in E_{CP} does not exceed the size of the corresponding symbol in Figure 5).

This analysis resulted in the classification of about 440 spectral lines in the 12.5–16 nm wavelength range, which belong to $4d^m - (4d^{m-1}4f + 4p^5 4d^{m+1})$ transitions in the spectra of Sn VIII–XIV ($m = 1-7$). Of prime interest for VUV lithography is the 2% wavelength interval near $\lambda = 13.5$ nm (13.5 ± 0.135 nm); this is precisely the interval that coincides with the reflection band of Mo/Si mirrors.

Figure 6 shows a portion of the spectrum of a vacuum spark (20 kV) in the 2% wavelength interval with reference of the most intense lines to their ionization stages. The spectrum of tin ions in the interval used for 13.5 nm lithography primarily consists of transitions in Sn XI–Sn XIII. Hence, we can draw a preliminary conclusion: obtaining an efficient

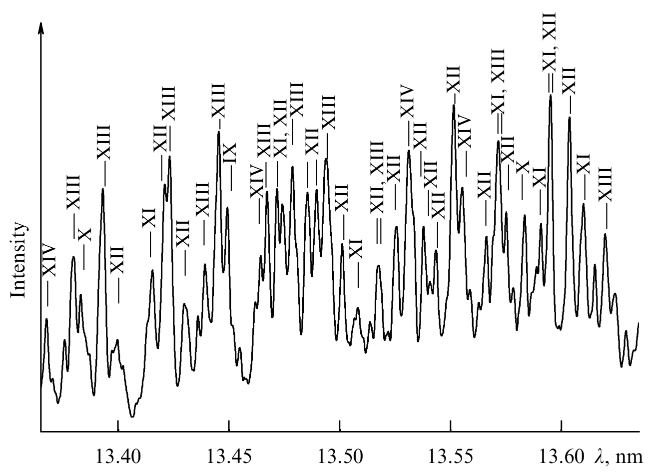

Figure 6. Classification of the spectral lines of tin in the 2% interval about the 13.5-nm wavelength by their ionization stages. (Borrowed from Ref. [26].)

radiation source in the interval $\lambda = 13.5 \pm 0.135$ nm requires producing a plasma with a prevalence of the ions Sn^{+10} – Sn^{+12}.

Similar investigations of the spectra of indium ions with the nuclear charge $Z_C = 49$ performed in parallel confirmed the main results of tin spectrum analysis ($Z_C = 50$). It was noted that the 4 – 4 transition spectra for different ionization degrees gradually separate in wavelength as the nuclear charge decreases. This is favorable to a more reliable classification of transitions in each specific ion. Presently underway in the Department of Atomic Spectroscopy of ISAN is an investigation of the 4 – 4 transition spectra in Pd, Ag, and Cd ions ($Z_C = 46 - 48$) intended to verify the results of our analysis of tin ionic spectra. Nevertheless, even now the data obtained are advantageously used as the spectroscopic foundation for modeling, development, and optimization of 13.5 nm lithography radiation sources based on tin ions.

Acknowledgements. This research was supported by the 6th Framework Program of the European Community (project IST-1-507754-IP), the Russian Foundation for Basic Research grants Nos 05-02-08224-ofi and 07-02-00244-a, and partly by the Optical Spectroscopy and Frequency Standards Program of the Physical Sciences Division, RAS.

References

1. Martin W C, Zalubas R, Hagan L, Natl. Stand. Ref. Data Ser. Natl. Bureau Stand. NSRDS-NBS 60 (Washington: National Bureau of Standards, 1978)
2. BIBL: Bibliography database on atomic spectra, http://das101.isan.troitsk.ru/bibl.htm
3. Biemont E, Palmeri P, Quinet P *Astrophys. Space Sci.* **269** 635 (1999); D.R.E.A.M. Database on Rare Earths at Mons University, http://w3.umh.ac.be/~astro/dream.shtml
4. Tolstikhina I Yu, Churilov S S, Ryabtsev A N, Koshelev K N, in *EUV Sources for Lithography* Vol. PM149 (Ed. V Bakshi) (Bellingham, Wash.: SPIE Press, 2006) p.113
5. Svendsen W, O'Sullivan G *Phys. Rev. A* **50** 3710 (1994)
6. Crosswhite H, Private communication (1976)
7. Aldenius M, Master Thesis (Lund: Depart. of Physics, Univ. of Lund, 2001)
8. Ryabchikova T, Ryabtsev A, Kochukhov O, Bagnulo S *Astron. Astrophys.* **456** 329 (2006)
9. Kochukov O, Ryabchikova T, Piskunov N *Astron. Astrophys.* **415** L13 (2004)
10. Cowan R D *The Theory of Atomic Structure and Spectra* (Berkeley: Univ. of California Press, 1981)
11. Wahlgren G M *Phys. Scripta* **T100** 22 (2002)
12. Biemont E, Quinet P *Phys. Scripta* **T105** 38 (2003)
13. Sugar J, Spector N *J. Opt. Soc. Am.* **64** 1484 (1974)
14. Den Hartog E A, Wickliffe M E, Lawler J E *Astrophys. J. Suppl.* **141** 255 (2002)
15. Ryabchikova T et al. *Astron. Astrophys.* **343** 229 (1999)
16. Wyart J F *J. Opt. Soc. Am.* **68** 197 (1978)
17. Wyart J F, Buache-Arnold Cl *Phys. Scripta* **22** 583 (1980)
18. Mashonkina L, Ryabchikova T, Ryabtsev A *Astron. Astrophys.* **441** 309 (2005)
19. Wyart J-F, Tchang-Brillet W-Ü L, Churilov S S, Ryabtsev A N *Astron. Astrophys.* **483** 339 (2008)
20. Churilov S S, Kildiyarova R R, Ryabtsev A N, Kramida A E, Joshi Y N *Phys. Scripta* **50** 463 (1994)
21. Azarov V I, Joshi Y N, Churilov S S, Ryabtsev A N *Phys. Scripta* **50** 642 (1994)
22. Sugar J, Kaufman V, Rowan W L *J. Opt. Soc. Am. B* **9** 1959 (1992)
23. Azarov V I, Joshi Y N *J. Phys. B* **26** 3495 (1993)
24. Churilov S S, Ryabtsev A N *Opt. Spektrosk.* **100** 721 (2006) [*Opt. Spectrosc.* **100** 660 (2006)]
25. Churilov S S, Ryabtsev A N *Opt. Spektrosk.* **101** 181 (2006) [*Opt. Spectrosc.* **101** 169 (2006)]
26. Churilov S S, Ryabtsev A N *Phys. Scripta* **73** 614 (2006)

PACS numbers: 03.75.Hh, 71.35.Lk, **71.36. + c**
DOI: 10.3367/UFNe.0179.200903k.0309

Strong correlations and new phases in a system of excitons and polaritons. A polariton laser

Yu E Lozovik

One of the most beautiful phenomena in many-particle physics — Bose–Einstein condensation (BEC) in a system of particles with nonzero mass m obeying the Bose statistics — was predicted by Einstein already in 1925 soon after the publication of Bose's paper on the thermodynamically equilibrium distribution of photons. Einstein showed that at a temperature T below the critical value

$$T_c = \frac{3.31\hbar^2}{m} n^{2/3} \tag{1}$$

(where n is the concentration of particles), the integral of the distribution function over all momenta decreases to below the total number of particles; in order to resolve this paradox, he assumed that all 'missing' particles lie in the one and only state with the lowest energy (and zero momentum). If $T \leqslant T_c$, the thermal de Broglie wavelength is of the order of the average distance between particles or is larger than it, such that the BEC occurs only in the quantum mode for a system of particles. If $T \to 0$, all particles in a system of noninteracting particles form the condensate.

After P Kapitza discovered the superfluidity of ^{4}He, F London suggested that superfluidity may stem from BEC. This was a brave hypothesis because BEC was then predicted only for noninteracting particles, while the interaction in condensed ^{4}He is strong. The BEC theory was generalized to the case of interacting particles only later (see [1–3] and the references therein). It was found that the interaction 'exhausts' the Bose condensate such that not more than 9% of particles in ^{4}He stay in the condensate even at $T \to 0$. This was shown by first-principle quantum Monte Carlo calcula-